Revisiting soliton dynamics in fiber optics under strict photon-number conservation

Nicolás Linale, Pablo I. Fierens, *Senior Member, IEEE,* and Diego F. Grosz

***Abstract*—We revisit the complex interplay between the Raman-induced frequency shift (RIFS) and the effect of self-steepening (SS) in the propagation of solitons, and in the framework of an equation that ensures strict conservation of the number of photons. The generalized nonlinear Schrödinger equation (GNLSE) is shown to severely fail in preserving the number of photons for sub-100-fs solitons, leading to a large overestimation of the frequency shift. Furthermore, when considering the case of a frequency-dependent nonlinear coefficient, the GNLSE also fails to provide a good estimation of the time shift experienced by the soliton. We tackle these shortcomings of the GNLSE by resorting to the recently introduced photon-conserving GNLSE (pcGNLSE) and study the interplay between the RIFS and self-steepening. As a result, we make apparent the impact of higher-order nonlinearities on short-soliton propagation and propose an original and direct method for the estimation of the second-order nonlinear coefficient.**

***Index Terms*—Nonlinear optics, Raman scattering, self-steepening.**

I. Introduction

INTRAPULSE Raman scattering is a nonlinear effect responsible for the redshift experienced by short optical pulses upon propagation in nonlinear waveguides. Usually referred to as the Raman-induced frequency shift (RIFS), it acts by transferring energy from high- to low-frequency components in the pulse spectrum, and its molecular origin is usually modeled by the inclusion of a retarded nonlinear response in the propagation equation [1]. As it is well known, RIFS becomes more apparent when dealing with sub-picosecond pulses, as the broad spectrum of the pulse is subjected to a Raman-gain gradient. This effect has been widely observed in experiments [2], [3], [4], [5]. In particular, RIFS is responsible for the soliton decay and redshift [6], with an ensuing time shift of the soliton enabled by the group-velocity dispersion (GVD) of the medium. This phenomenon of soliton self-frequency shift finds application in many areas of optics and photonics, such as in frequency-tunable femtosecond sources [7], signal processing, and tunable time delays, among others [8].

Another relevant effect in the realm of short pulses is that of self-steepening (SS), which is responsible for the shock of optical pulses and is modeled by considering a linear frequency dependence of the nonlinear coefficient of the supporting waveguide [1]. In the context of solitons, and most remarkably, self-steepening induces a time shift without the occurrence of an optical shock [9], [10]. Specifically, the SS parameter, s_1, is related to the first-order term of the Taylor expansion of the nonlinear coefficient $\gamma(\Omega) = \gamma_0\,(1 + s_1 \frac{\Omega}{\omega_0})$, where ω_0 is the pulse central frequency, $\Omega = \omega - \omega_0$ is the frequency detuning from ω_0, and $s_1 \doteq \frac{\omega_0}{\gamma_0}\gamma_1$, i.e., s_1 is a dimensionless normalization of γ_1. The SS parameter acquires particular relevance when modeling highly nonlinear broadband processes such as in the case of supercontinuum generation (SCG) [11], [12]. The complex interplay between these effects, RIFS and SS, has already been studied in the literature (see, e.g., [13]) and is the focus of this paper.

Light-pulse propagation in waveguides is usually modeled by the nonlinear Schrödinger equation (NLSE) [1]. However, it must be emphasized that if the SS parameter differs from $s_1 = 1$, the NLSE fails in general to preserve the energy and the photon number in lossless media [14], [15], [16], a fact oftentimes overlooked in the literature on the subject. Frequency-dependent nonlinear profiles can be found in many kinds of waveguides, such as photonic crystal fibers (PCF), chalcogenide fibers, silicon waveguides, decorated silicon waveguides, and doped waveguides, among many other relevant guiding media [11], [17], [18], [19]. Indeed, let us recall that $\gamma(\Omega) = (\Omega + \omega_0)n_2/cA_{\text{eff}}$, where n_2 is the nonlinear refractive index, c is the speed of light, and A_{eff} is the effective mode area. The particular case $s_1 = 1$ (or equivalently $\gamma_1 = \gamma_0/\omega_0$) implies that the quotient n_2/A_{eff} must not depend on frequency. However, since $A_{\text{eff}} = A_{\text{eff}}(\Omega)$ and $n_2 = n_2(\Omega)$, this assumption does not normally hold. For instance, in the work of Zhao et al. [17], values of s_1 as large as ± 42 are found.

When the effect of Raman scattering is included into the NLSE the resulting equation, called generalized nonlinear Schrödinger equation (GNLSE), no longer conserves energy as there is a transfer from the electromagnetic field to the material medium. Thus, in this case it is customary to look at the evolution of the number of photons instead of energy as a measure of the validity of the numerical results. Unfortunately, as with the NLSE, the GNLSE fails to conserve the number of photons for $s_1 \neq 1$. Furthermore, this equation only predicts physically sound results when positive zeroth-order nonlinear coefficients (γ_0) are taken into account. For negative coefficients, however, the GNLSE predicts an unphysical blueshift of short pulses [20], [21], a problem worsened when the SS parameter departs from the photon-conserving condition $s_1 = 1$ of the GNLSE.

In view of these considerations, the GNLSE is not suitable

N. Linale and D.F. Grosz are with the Depto. de Ingeniería en Telecomunicaciones, Centro Atómico Bariloche, GDTyPE, GAIyANN, Comisión Nacional de Energía Atómica, Río Negro 8400, Argentina.

P. I. Fierens is with the Centro de Optoelectrónica, Instituto Tecnológico de Buenos Aires (ITBA), CABA 1106, Argentina.

All three authors are with the Consejo Nacional de Investigaciones Científicas y Técnicas (CONICET), Argentina.

to study the complex interplay between RIFS and SS in short pulses, where the influence of the self-steepening parameter is of the utmost relevance. Indeed, such study requires a modeling equation that can accommodate an arbitrary frequency-dependent nonlinear coefficient (e.g., with $s_1 \neq 1$), while preserving the mean photon number. To tackle this issue, we have derived a modified GNLSE, the photon-conserving generalized nonlinear Schrödinger equation (pcGNLSE) [21], an equation that ensures that the photon number is conserved in lossless media. Analyses in this work are, thus, based on the pcGNLSE.

Finally, it is important to emphasize that, to the very best of our knowledge, only a linear frequency-dependent $\gamma(\Omega)$ is assumed for modeling purposes in the literature. Indeed, it has been shown that such approximation form is sufficient for most purposes, even in the case of few-cycle pulses (see, e.g., [22]). Nonetheless, some waveguides exhibit a more complex frequency dependence of the nonlinearity [23], [24], [25], [18]. This fact motivates the question of whether such complex dependence can be observed in experiments and how it can be measured. In this work, we provide some insight into this matter by exploring the influence of the second-order term of the Taylor expansion of $\gamma(\Omega)$ on the time delay experienced by short solitons.

The rest of the paper is organized as follows: In Section II, we review how RIFS and SS perturb a soliton in the long-pulse regime ($\geq$ 100 fs), as modeled by the GNLSE and pcGNLSE. Then, in Section. III, we analyze short pulses with both equations and show the former to predict the gain or loss of photons depending upon the magnitude of the self-steepening parameter. In Section IV we analyze the influence of the second-order term of the Taylor expansion of the nonlinear coefficient, γ_2, and propose an original method to estimate it from measurements. Final remarks are presented in Section V.

II. Evolution of long pulses

Let us first review the behavior of long soliton pulses under the generalized nonlinear Schrödinger equation [1]

$$\frac{\partial \tilde{A}_\omega}{\partial z} = i\beta(\omega)\tilde{A}_\omega + i\gamma(\omega)\mathcal{F}\left\{A|A|^2\right\} + if_{\mathrm{R}}\gamma(\omega)\mathcal{F}\left\{A\int_0^\infty h(\tau)|A(t-\tau)|^2 d\tau - A|A|^2\right\}, \quad (1)$$

where $A = A(z,t)$ is the complex envelope of the electric field in the time domain, normalized such that $|A|^2$ is the optical power, and $\tilde{A} = \tilde{A}(z,\omega) = \mathcal{F}[A(z,t)]$, $\mathcal{F}$ standing for the Fourier transform. Coefficients $\beta(\omega)$ and $\gamma(\omega)$ are the linear and nonlinear dispersion profiles, respectively, and it is customary to express these profiles as Taylor expansions. Function $h(t)$ accounts for the delayed Raman response and f_{R} is the fractional Raman contribution.

Solitons in optical waveguides have been studied for several decades (see, e.g., [26], [27] and references therein.) Let us briefly recall that, in the absence of higher-order linear and nonlinear dispersion and Raman scattering, these solutions are characterized by the integer N, called the 'soliton order', given by $N^2 = \gamma_0 P_0 T_0^2/|\beta_2|$, where γ_0 is the zeroth-order nonlinear coefficient, β_2 is the group velocity dispersion parameter of the waveguide, and P_0 and T_0 are the soliton peak power and $1/e$ half width, respectively [28]. The influence of higher-order linear and nonlinear dispersion and Raman scattering on the propagation of solitons can be analyzed by the method of moments [29], [30], [13], [1] (for an alternative approach to the analysis of soliton perturbations see, e.g., [31]). This method posits the ansatz

$$A(z,T) = a_p \mathrm{sech}\left(\frac{T-q_p}{T_p}\right) \exp\left\{-i\Omega_p(T-q_p) - iC_p\frac{(T-q_p)^2}{2T_p^2} + i\phi_p\right\}, \quad (2)$$

where a_p, T_p, C_p, q_p, Ω_p, and ϕ_p stand for the amplitude, width, chirp, time shift, frequency shift, and the soliton phase, respectively; note that the latter can be neglected without any loss of generality and that, for short propagation distances, the width remains nearly constant and the chirp is null.

Neglecting higher-order dispersion terms and introducing an effective Raman parameter T_{R} [1], it can be shown that the frequency and time shifts are given by [29], [30]

$$\Omega_p(z) = -\frac{8T_{\mathrm{R}}\gamma_0 P_0}{15T_0^2}z, \qquad q_p(z) = \frac{\beta_2\Omega_p}{2}z + \frac{s_1\gamma_0 P_0}{\omega_0}z. \quad (3)$$

Since T_{R} is positive, the spectrum experiences a redshift when $\gamma_0 > 0$. If, however, $\gamma_0 < 0$ (as in some types of waveguides [23], [32], [33]), Eq. (3) predicts an unphysical increase of the soliton energy [20], [21], a drawback that stems from applying the GNLSE to model propagation in the presence of arbitrary nonlinearity profiles. In what follows we will assume that $\gamma_0 > 0$.

The first term of $q_p(z)$ in Eq. (3) accounts for the delay induced by Raman where the GVD parameter, β_2, turns the RIFS into an effective group velocity; the second term is due to self-steepening. Figure 1 (left) shows the propagation of a 100-fs soliton at 1550 nm along 100 L_{D} in a fiber with $\beta_2 = -20$ ps^2/km, $\gamma_0 = 1$ W^{-1}km^{-1}, and $s_1 = -1$, where $L_{\mathrm{D}} = T_0^2/|\beta_2|$ is the dispersion length. The Raman response of the medium is modeled as $h(t) = (\tau_1^{-2} + \tau_2^{-2})\tau_1 \exp(-t/\tau_2)\sin(t/\tau_1)$, with $\tau_1 = 12.2$ fs, $\tau_2 = 32$ fs, and $f_R = 0.18$ [1], [14]. Henceforth, the effect of attenuation is neglected in the simulations, as the propagation distances considered are much shorter than the corresponding attenuation characteristic length. Top and middle panels show the normalized time and frequency shifts, respectively. As it can be observed, simulation results are in excellent agreement with results from Eq. (3), shown in dashed lines. The bottom panel in Fig. 1 shows, for the GNLSE, a slight increase in the photon number with distance due to $s_1 \neq 1$. This deviation is small because of the weak effect of self-steepening when considering long pulses. Let us note that the photon number is calculated as $\int_0^{+\infty} |\tilde{A}|^2/(\hbar\omega)d\omega$.

The failure of the GNLSE to conserve the number of photons motivated us to introduce the photon-conserving GNLSE

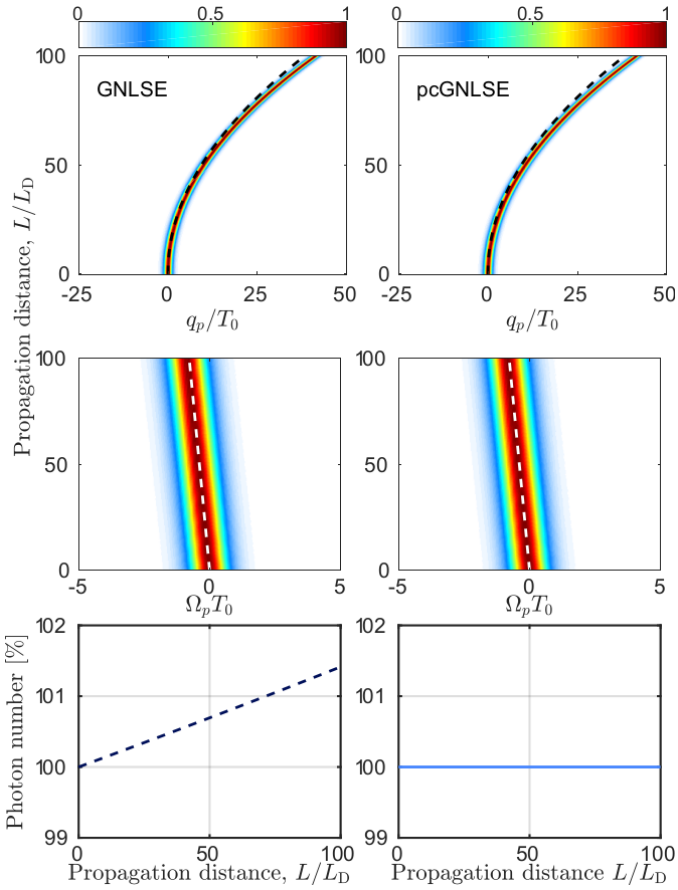

Fig. 1. (Top) Time and (center) frequency shifts experienced by 100-fs solitons along 100 L_D in a waveguide with $s_1 = -1$, as predicted by the GNLSE (left) and the pcGNLSE (right). (Bottom) Photon-number evolution. Dashed lines show results from Eqs. (3) and (5) in excellent agreement with simulations.

(pcGNLSE), which reads [21]

$$\frac{\partial \tilde{A}_\omega}{\partial z} = i\beta(\omega)\tilde{A}_\omega + i\frac{\overline{\gamma}(\omega)}{2}\mathcal{F}\left(C^* B^2\right) + i\frac{\overline{\gamma}^*(\omega)}{2}\mathcal{F}\left(B^* C^2\right) + if_R\overline{\gamma}^*(\omega)\mathcal{F}\left(B\int_0^\infty h(\tau)|B(t-\tau)|^2 d\tau - B|B|^2\right), \quad (4)$$

where $\overline{\gamma}(\omega) = \omega\tilde{r}$, $\tilde{B} = \tilde{r}\tilde{A}$, $\tilde{C} = \tilde{r}^*\tilde{A}$, and $\tilde{r} = \sqrt[4]{\gamma(\omega)/\omega}$. This equation was derived based on quantum mechanical considerations. Without going into details, which the interested reader can find in full in Ref. [21] and references therein, the key point of the derivation is the introduction of an adequate quantum Kerr operator. In particular, in the pcGNLSE the derivation of such operator is motivated by the validity of a generalized Miller's rule for the nonlinear susceptibility [34], which has been shown to be accurate for a broad range of media (see e.g. [35]). Miller's rule implies a relation between the third- and first-order susceptibilities: $\chi^{(3)}_{\omega_1,\omega_2,\omega_3,\omega_4} \propto \chi^{(1)}_{\omega_1}\chi^{(1)}_{\omega_2}\chi^{(1)}_{\omega_3}\chi^{(1)}_{\omega_4}$, and this is the reason behind the fourth root in the definition of $\tilde{r}(\omega)$.

Although Eq. (4) appears to be more complex than the GNLSE, it can be solved with the very same numerical methods, e.g., the split-step Fourier method [36]. Furthermore, it can be shown that the pcGNLSE reduces to the GNLSE whenever $s_1 = 1$, that is, in the only case where the latter conserves the photon number. It is worth mentioning that the pcNLSE, i.e., a similar equation to the pcGNLSE but neglecting the delayed Raman response of the medium, has already been successfully applied to the study of modulation instability in waveguides with frequency-dependent nonlinear coefficients [37], in the modeling of broadband two-photon absorption [38], and in the study of nonlinear phenomena in waveguides doped with metal nanoparticles [39]. In this paper, we make use of the pcGNLSE to focus on the influence of Raman scattering, self-steepening, and high-order nonlinearity on soliton propagation within the framework of the strict conservation of the number of photons.

As with the GNLSE, we start our analysis from Eq. (2) and the method of moments. For long pulses, Eq. (4) can be approximated up to a first order in Ω/ω_0. Proceeding this way and modeling the influence of Raman by introducing T_R, it can be shown that Raman plays exactly the same role in the pcGNLSE as it does in the GNLSE. This might have been expected, since we deal with long pulses and similar approximations. However, self-steepening plays a different role in the pcGNLSE as this equation guarantees the conservation of the photon number for any value of s_1.

Using the method of moments with this equation, it can be proved that, for $\gamma_0 > 0$, the frequency and time shifts are given by (see Appendix A for details)

$$\Omega_p(z) = -\frac{8T_R\gamma_0 P_0}{15T_0^2}z, \quad q_p(z) = \frac{\beta_2\Omega_p}{2}z + \frac{(s_1+2)\gamma_0 P_0}{3\omega_0}z. \quad (5)$$

Comparing Eq. (5) to Eq. (3), we see that they predict the same RIFS. However, they differ in the way they account for the influence of self-steepening on the delay experienced by the soliton. Most remarkably, and as predicted by the pcGNLSE, *the effect of SS vanishes when* $s_1 = -2$. Note the linear relation between q_p and s_1; this relation can be used to obtain the SS parameter by measuring the delay, as it was proposed in Ref. [40]. Figure 1 (right) shows the evolution of a 100-fs soliton as simulated with the pcGNSLE. As it can be readily seen, the photon number remains constant along propagation. In the long-pulse regime, both the GNLSE and the pcGNLSE predict similar results in excellent agreement with analytical predictions in direct correlation with the small photon gain observed in the GNLSE, and a signature of a long-pulse regime.

In what follows we will focus on the short-pulse regime, where the enhanced influence of self-steepening and higher-order nonlinearities are shown to have profound consequences on the soliton evolution, as obtained with the two modeling equations.

III. Evolution of Short Pulses

Time and frequency shifts given by Eqs. (3) and (5) are valid for unchirped solitons with constant width and peak power. In the case of short pulses ($T_0 < 100$ fs), however, these conditions are not maintained upon propagation. Moreover, the effective Raman parameter T_R becomes dependent on the pulse width [13]. In order to illustrate this scenario, Fig. 2

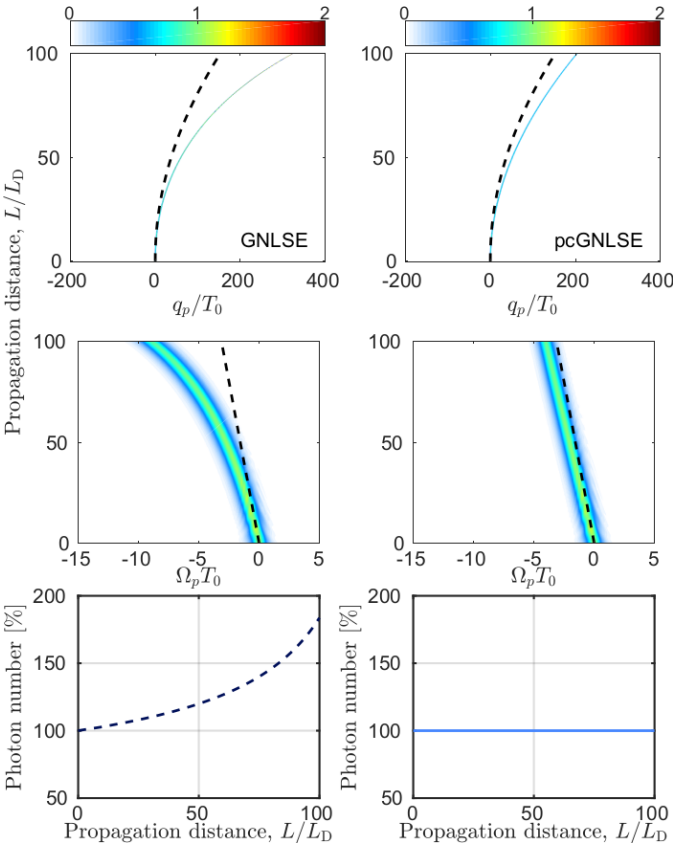

Fig. 2. (Top) Time and (center) frequency shifts experienced by 25-fs solitons along 100 L_D in a waveguide with $s_1 = -1$, as predicted by the GNLSE (left) and the pcGNLSE (right). (Bottom) Photon-number evolution. Black-dashed lines show results from Eqs. (3) and (5).

shows the propagation of a 25-fs soliton along a fiber with the same parameters of those in Fig. 1, with both the GNLSE and the pcGNLSE. Note that the soliton peak power is normalized to its initial value as $P(z)/P_0$. As it can be observed, the GNLSE and the pcGNLSE predict very different outcomes, i.e., the former leads to a much larger RIFS and an ensuing larger delay, while displaying an unphysical surge in the number of photons. The pcGNLSE, however, predicts smaller frequency and time shifts, while observing strict conservation of the number of photons along propagation. Black-dashed lines show analytical results from Eqs. (3) and (5) that do not match the numerical results. Observe that the GNLSE leads to a large overestimation of the RIFS in direct relation with the non-conservation of the photon number, a characteristic made more apparent in the case of short pulses with broader spectra (compare results from Figs. 1 and 2.)

To further show the correlation between results obtained with the GNLSE and the pcGNLSE, and the photon number evolution, we study the dependence of the time delay, frequency shift, and photon number on the self-steepening parameter. Results for a 25-fs soliton at a propagated $15\,L_D$ are shown in Fig. 3. A direct correlation between an increase in photon number and a larger time- and frequency-shift is readily observed. Note that, as expected, when $s_1 = 1$ the GNLSE conserves the photon number. However, for a larger SS parameter the GNLSE predicts a slight loss of photons.

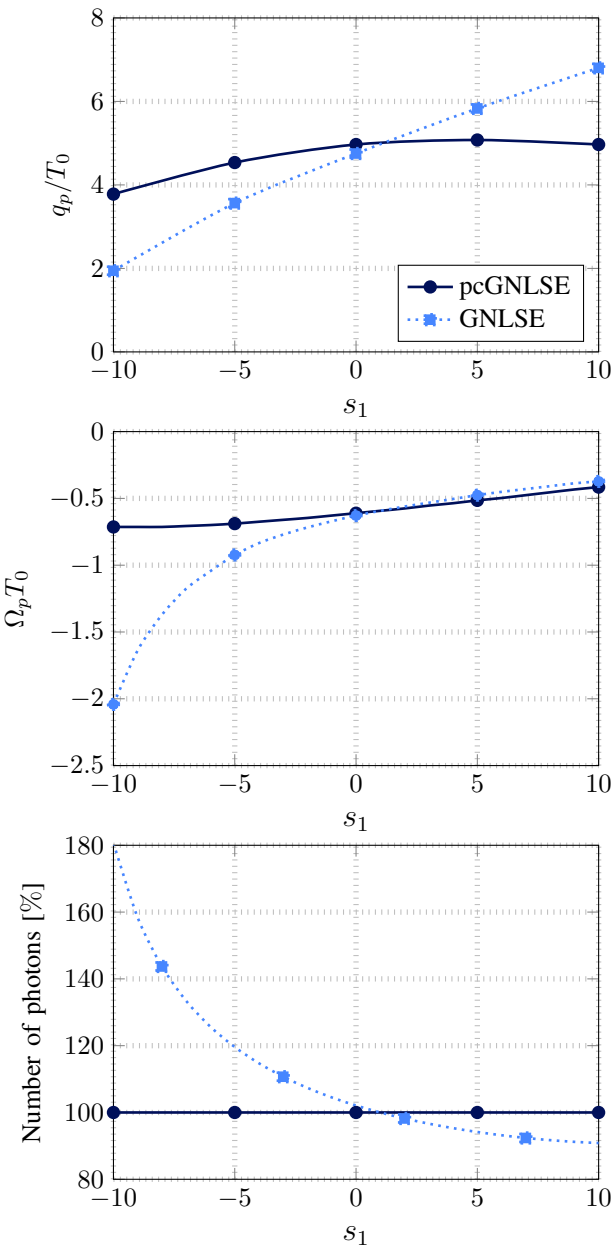

Fig. 3. (Top) Time and (center) frequency shifts experienced by 25-fs solitons along 15 L_D, as predicted by the pcGNLSE (circles) and GNLSE (squares), for different SS parameters. (Bottom) Photon-number evolution.

Since the difference is considerably smaller as compared to cases with $s_1 < 1$, the predicted frequency and time shifts approach those obtained with the pcGNLSE. In physical terms, this asymmetric behavior of the GNLSE around $s_1 = 1$ can be explained by the appearance of a zero-nonlinearity wavelength (ZNW) in the low-frequency side of the spectrum, for $s_1 > 0$, that limits the RIFS [20].

IV. Higher-order nonlinearities

As we have already mentioned, the literature usually focuses on the expansion of $\gamma(\Omega)$ only up to the first order, even when dealing with the modeling of intrinsic broadband highly nonlinear processes such as supercontinuum generation [12].

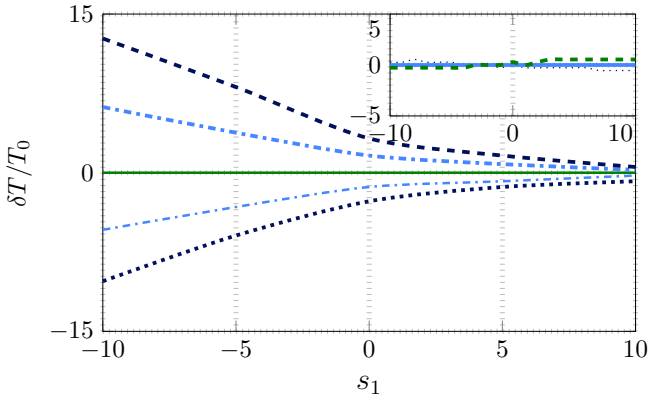

Fig. 4. Normalized relative time shift experienced by 10-fs solitons propagated along 45 $L_{\rm D}$, vs. s_1 and for (bottom to top) $s_2 = -10$, -5, 0, 5, and 10. Time shifts are measured relative to that obtained for $s_2 = 0$. (Inset) Same but neglecting Raman scattering.

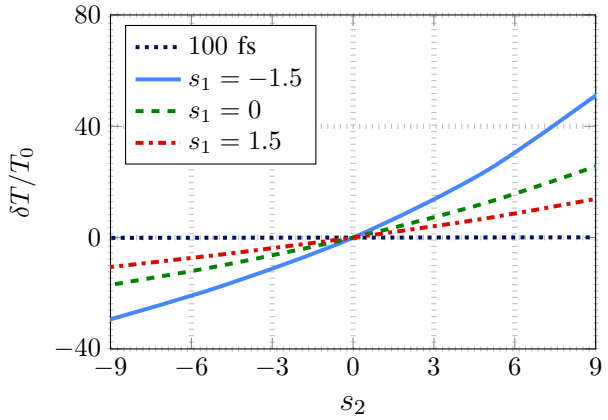

Fig. 5. Relative time shift vs. s_2 experienced by short 10-fs solitons, and for different s_1. The horizontal dotted line corresponds to long 100-fs solitons.

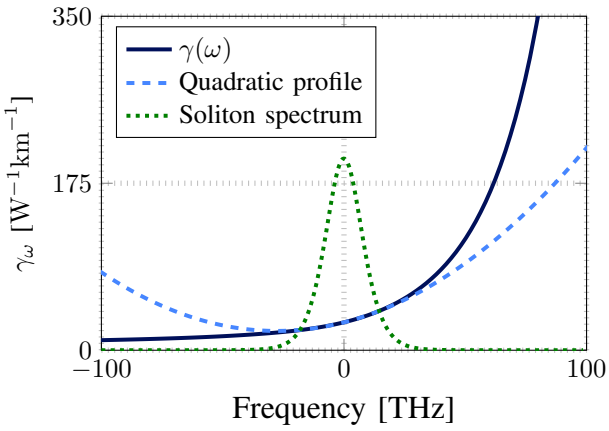

Fig. 6. Nonlinear profile of a waveguide doped with Au nanoparticles (solid line) and quadratic approximation around $\omega = \omega_0$ (dashed line). The 10-fs soliton spectrum is shown with a dotted line for reference. $\gamma_0 = 30$ W^{-1}km^{-1}, $s_1 = 7.86$, and $s_2 = 100.03$.

In this section we focus on the effect that higher-order nonlinearity has on the propagation of short solitons. Bear in mind that such task can only be performed by resorting to the pcGNLSE as, it was shown in the previous section, the GNLSE in general fails to conserve the photon number and hence it does not yield reliable results.

Let us define s_2 such that $\gamma(\Omega) = \gamma_0\,(1 + s_1\frac{\Omega}{\omega_0} + s_2\frac{\Omega^2}{2\omega_0^2})$. Figure 4 shows that the effect of s_2 can be revealed by measurable variations in the time delay experienced by a 10-fs soliton, as the delay depends not only on the self-steepening parameter s_1, but also on the second-order parameter s_2. For the sake of clarity, Fig. 4 shows a relative time shift δT, defined as $\delta T = q_p(s_1, s_2) - q_p(s_1, 0)$, i.e., the deviation with respect to the delay for $s_2 = 0$. It is worthwhile pointing out that Raman scattering acts as an enabler of the higher-order nonlinearity. Indeed, when switching off the Raman contribution the delay no longer depends on s_2, as shown in the inset of Fig. 4.

Measurement of soliton dynamics can be used to estimate fiber parameters [41], [40]. Indeed, the dependence of the time shift on the higher-order nonlinear coefficient s_2, as observed in Fig. 4, suggests a way for its estimation. The underlying idea of this proposal is presented in Fig. 5, where the relative time delay vs. s_2 is shown for three different SS parameters $s_1 = -1.5, 0, 1.5$. In all cases, it is verified that the delay is unaffected in the case of long 100-fs pulses. Shorter 10-fs pulses, however, experience a delay that depends monotonically on s_2. A practical implementation of a scheme to measure s_2 will first require the measurement of the time delay experienced by a long soliton to obtain s_1 [40]. Then, the propagation of a short soliton will make apparent the influence of the higher-order nonlinearity on the delay.

In order to demonstrate the proposed measurement scheme for s_1 and s_2, let us consider its application to a complex nonlinear profile such as that encountered in waveguides doped with Au nanoparticles. Figure 6 shows an example of such a profile (solid line), taken from Ref. [39], centered around $\omega_0 = 2\pi c/\lambda_0$, with $\lambda_0 = 850$ nm. We simulate the proposed measurement scheme, assuming that β_2 ($= -100$ ps^2/km) and γ_0 ($= 30$ W^{-1}km^{-1}) are known, and that Raman parameters are those of fused silica, i.e., the host material [20]. First, we launch a 100-fs fundamental soliton in order to find s_1. Figure 7 (left) shows the input and output pulses after 30 $L_{\rm D}$, where it is found that the time shift is 4.12 T_0 whence the estimated SS parameter is $\hat{s}_1 = 7.64$. Second, a short 10-fs soliton is propagated along 30 $L_{\rm D}$. Here, the observed time shift is 17.10 T_0 (see the bottom panel of Figure 7). In order to estimate s_2, we perform numerical simulations using the estimated value of $\hat{s}_1$ and for different values of s_2: 30, 60, 90, and 120. Each of these simulations predicts a different time delay, as illustrated in Fig. 8 (squares). Interpolating these results, we estimate $\hat{s}_2 = 86$ (marked with a red dot). We can compare results of the simulated estimation procedure with those of the quadratic approximation of the nonlinear profile shown in Fig. 6 (dashed line): $s_1 = 7.86$, and $s_2 = 100.03$. As such, the relative errors incurred in the estimation of s_1 and s_2 are $\sim 3\%$ and $\sim 14\%$, respectively. All things considered, the proposed scheme allows for a good estimation of the higher-order nonlinearity.

It is important to note that the input pulse wavelength

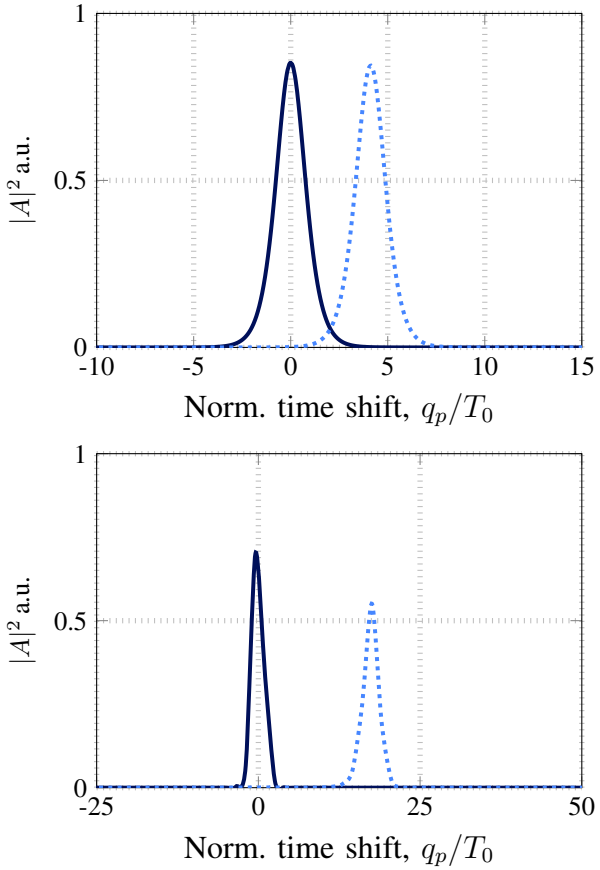

Fig. 7. Time shift experienced by (top) 100-fs and (bottom) 10-fs solitons when traversing the doped waveguide. (Solid line) Input soliton, (dotted line) output soliton.

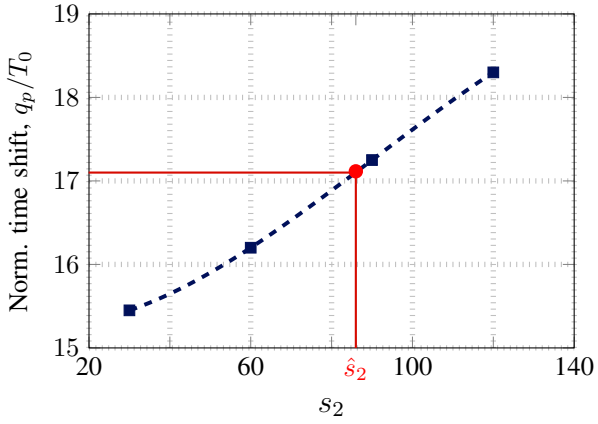

Fig. 8. Normalized time shift q_p/T_0 vs. s_2. Simulations for $s_2 = 30$, 60, 90, and 120 (blue squares) and interpolated results (dashed line). The red dot marks the value of s_2 estimated for the doped waveguide.

must be far apart from the plasmon resonance of the doping inclusion in order to avoid excessive absorption. We refer the interested reader to Ref. [39] for a discussion on this topic in doped waveguides. Even though this is the case in this example, the waveguide is longer than the effective attenuation distance. The influence of the attenuation, which was neglected in order to emphasize the effect of the higher-order nonlinearity, can nonetheless be incorporated into the pcGNLSE in straightforward fashion. Furthermore, two-photon (nonlinear) absorption can also be accounted for within the framework of the pcGNLSE as shown in Ref. [38].

V. Conclusions

In summary, we revisited the complex interplay between the Raman-induced frequency shift, self-steepening, and higher-order nonlinearity in the propagation of short solitons. We showed that, for sub-100-fs solitons, the GNLSE fails in preserving the number of photons, leading to a large overestimation of the frequency and time shifts experienced by the pulse. These shortcomings motivated the need to resort to an adequate photon-conserving propagation equation such as the pcGNLSE.

We also showed that the time shift suffered by short solitons is a harbinger of higher-order nonlinearity. This realization motivated us to propose an original and direct method to estimate the second-order nonlinear coefficient of the waveguide. Finally, and in view of the results presented, we emphasize the need to account for the higher-order nonlinearity when dealing with the propagation of short pulses in waveguides and all associated phenomena. The effects of higher-order nonlinearity are most certainly present in various experiments but the scientific community did not have the right tool, until now, to correctly model the influence of arbitrary nonlinear profiles. As such, the pcGNLSE may shed new light on the problem of propagation in media with new and exciting nonlinear properties.

Appendix A
Time and Frequency Shifts for the pcGNLSE

Let us assume that $\gamma(\Omega) > 0$. In this case, $\tilde{C} = \tilde{B}$ and the pcGNLSE can be written as

$$\frac{\partial \tilde{A}}{\partial z} = i\beta(\Omega)\tilde{A}(z,\Omega) + if_{\mathrm{R}}\overline{\gamma}(\omega)\mathcal{F}\left\{B(z,t)\int_0^\infty R(t')|B(z,t-t')|^2dt'\right\}, \quad (6)$$

where

$$R(t) = (1-f_{\mathrm{R}})\delta(t) + f_{\mathrm{R}}h(t). \quad (7)$$

Eq. (6) can be expressed in terms of $B(z,t)$ only:

$$\frac{\partial \tilde{B}}{\partial z} = i\beta(\Omega)\tilde{B}(z,\Omega) + i\sqrt{(\omega_0+\Omega)\gamma(\Omega)}\times \mathcal{F}\left\{B(z,t)\int_0^\infty R(t')|B(z,t-t')|^2dt'\right\}. \quad (8)$$

If $\gamma(\Omega) = \gamma_0\left(1 + s_1\frac{\Omega}{\omega_0}\right)$, then

$$\sqrt{(\omega_0+\Omega)\gamma(\Omega)} \approx \sqrt{\gamma_0\omega_0}\left(1 + \frac{s_1+1}{2}\frac{\Omega}{\omega_0}\right), \quad (9)$$

where we have kept terms up to a first order in Ω/ω_0. Using this result and neglecting higher-order dispersion terms,

$$\frac{\partial B}{\partial z} = -i\frac{\beta_2}{2}\frac{\partial^2 B}{\partial t^2} + i\sqrt{\gamma_0\omega_0}\left(1 - i\frac{s_1+1}{2\omega_0}\frac{\partial}{\partial t}\right)\left(B(z,t)\int_0^\infty R(t')|B(z,t-t')|^2 dt'\right). \quad (10)$$

As it can be readily seen, this equation has the same functional form as the GNLSE. Furthermore, it is straightforward to show that, if $A(z,0)$ is a *sech* pulse with half-width T_0, then $B(z,0)$ has approximately the same amplitude for $\omega_0 T_0 \ll 1$. This fact explains why the Raman-induced frequency shift predicted by the pcGNLSE is the same as that obtained with the GNLSE for long pulses. The first term of the time shift in Eq. 5, due GVD and RIFS, is explained in the same manner. The second term of q_p in Eq. 5 has already been explained in Ref. [40], where the time shift of solitons was studied in the absence of Raman scattering.

REFERENCES

[1] G. P. Agrawal, *Nonlinear Fiber Optics*. Academic Press, 2013.

[2] F. M. Mitschke and L. F. Mollenauer, "Discovery of the soliton self-frequency shift," *Optics Letters*, vol. 11, no. 10, pp. 659–661, 1986.

[3] Q. Lin and G. P. Agrawal, "Raman response function for silica fibers," *Optics Letters*, vol. 31, no. 21, pp. 3086–3088, 2006.

[4] X. Liu, C. Xu, W. Knox, J. Chandalia, B. Eggleton, S. Kosinski, and R. Windeler, "Soliton self-frequency shift in a short tapered air–silica microstructure fiber," *Optics Letters*, vol. 26, no. 6, pp. 358–360, 2001.

[5] B. Washburn, S. E. Ralph, P. A. Lacourt, J. Dudley, W. T. Rhodes, R. S. Windeler, and S. Coen, "Tunable near-infrared femtosecond soliton generation in photonic crystal fibres," *Electronics Letters*, vol. 37, no. 25, pp. 1510–1512, 2001.

[6] G. P. Agrawal, "Effect of intrapulse stimulated Raman scattering on soliton-effect pulse compression in optical fibers," *Optics Letters*, vol. 15, no. 4, pp. 224–226, 1990.

[7] M. E. Masip, A. A. Rieznik, P. G. König, D. F. Grosz, A. V. Bragas, and O. E. Martinez, "Femtosecond soliton source with fast and broad spectral tunability," *Optics Letters*, vol. 34, no. 6, pp. 842–844, 2009.

[8] J. H. Lee, J. van Howe, C. Xu, and X. Liu, "Soliton self-frequency shift: experimental demonstrations and applications," *IEEE Journal of Selected Topics in Quantum Electronics*, vol. 14, no. 3, pp. 713–723, 2008.

[9] K. Ohkuma, Y. H. Ichikawa, and Y. Abe, "Soliton propagation along optical fibers," *Optics Letters*, vol. 12, no. 7, pp. 516–518, 1987.

[10] J. R. De Oliveira, M. A. de Moura, J. M. Hickmann, and A. S. L. Gomes, "Self-steepening of optical pulses in dispersive media," *Journal of the Optical Society of America B*, vol. 9, no. 11, pp. 2025–2027, 1992.

[11] B. Kibler, J. M. Dudley, and S. Coen, "Supercontinuum generation and nonlinear pulse propagation in photonic crystal fiber: influence of the frequency-dependent effective mode area," *Applied Physics B*, vol. 81, no. 2-3, pp. 337–342, 2005.

[12] B. Barviau, B. Kibler, and A. Picozzi, "Wave-turbulence approach of supercontinuum generation: Influence of self-steepening and higher-order dispersion," *Physical Review A*, vol. 79, no. 6, p. 063840, 2009.

[13] Z. Chen, A. J. Taylor, and A. Efimov, "Soliton dynamics in non-uniform fiber tapers: analytical description through an improved moment method," *Journal of the Optical Society of America B*, vol. 27, no. 5, pp. 1022–1030, 2010.

[14] K. J. Blow and D. Wood, "Theoretical description of transient stimulated Raman scattering in optical fibers," *IEEE Journal of Quantum Electronics*, vol. 25, no. 12, pp. 2665–2673, 1989.

[15] A. D. Sánchez, P. I. Fierens, S. M. Hernandez, J. Bonetti, G. Brambilla, and D. F. Grosz, "Anti-Stokes Raman gain enabled by modulation instability in mid-IR waveguides," *Journal of the Optical Society of America B*, vol. 35, no. 11, pp. 2828–2832, Nov 2018.

[16] A. Zheltikov, "Optical shock wave and photon-number conservation," *Physical Review A*, vol. 98, no. 4, p. 043833, 2018.

[17] S. Zhao and X. Sun, "Soliton dynamics in an all-normal-dispersion photonic crystal fiber with frequency-dependent Kerr nonlinearity," *Physical Review A*, vol. 102, no. 3, p. 033514, 2020.

[18] F. Arteaga-Sierra, A. Antikainen, and G. P. Agrawal, "Soliton dynamics in photonic-crystal fibers with frequency-dependent Kerr nonlinearity," *Physical Review A*, vol. 98, no. 1, p. 013830, 2018.

[19] A. Ishizawa, R. Kou, T. Goto, T. Tsuchizawa, N. Matsuda, K. Hitachi, T. Nishikawa, K. Yamada, T. Sogawa, and H. Gotoh, "Optical nonlinearity enhancement with graphene-decorated silicon waveguides," *Scientific R—eports*, vol. 7, p. 45520, 2017.

[20] S. Bose, A. Sahoo, R. Chattopadhyay, S. Roy, S. K. Bhadra, and G. P. Agrawal, "Implications of a zero-nonlinearity wavelength in photonic crystal fibers doped with silver nanoparticles," *Physical Review A*, vol. 94, no. 4, p. 043835, 2016.

[21] J. Bonetti, N. Linale, A. D. Sánchez, S. M. Hernández, P. I. Fierens, and D. F. Grosz, "Photon-conserving generalized nonlinear Schrödinger equation for frequency-dependent nonlinearities," *Journal of the Optical Society of America B*, vol. 37, no. 2, pp. 445–450, 2020.

[22] N. Karasawa, S. Nakamura, N. Nakagawa, M. Shibata, R. Morita, H. Shigekawa, and M. Yamashita, "Comparison between theory and experiment of nonlinear propagation for a-few-cycle and ultrabroadband optical pulses in a fused-silica fiber," *IEEE Journal of Quantum Electronics*, vol. 37, no. 3, pp. 398–404, 2001.

[23] S. Wen, Y. Wang, W. Su, Y. Xiang, X. Fu, and D. Fan, "Modulation instability in nonlinear negative-index material," *Physical Review E*, vol. 73, no. 3, p. 036617, 2006.

[24] S. Wen, Y. Xiang, W. Su, Y. Hu, X. Fu, and D. Fan, "Role of the anomalous self-steepening effect in modulation instability in negative-index material," *Optics Express*, vol. 14, no. 4, pp. 1568–1575, 2006.

[25] S. Wen, Y. Xiang, X. Dai, Z. Tang, W. Su, and D. Fan, "Theoretical models for ultrashort electromagnetic pulse propagation in nonlinear metamaterials," *Physical Review A*, vol. 75, no. 3, p. 033815, 2007.

[26] A. Hasegawa, F. Tappert, L. F. Mollenauer, R. H. Stolen, and L. P. Gordon, "Experimental observation of pico second pulse narrowing and solitons in optical fiber," *Applied Physics Letters*, vol. 23, p. 142, 1973.

[27] L. F. Mollenauer, R. H. Stolen, and J. P. Gordon, "Experimental observation of picosecond pulse narrowing and solitons in optical fibers," *Physical Review Letters*, vol. 45, no. 13, p. 1095, 1980.

[28] J. Satsuma and N. Yajima, "B. initial value problems of one-dimensional self-modulation of nonlinear waves in dispersive media," *Progress of Theoretical Physics Supplement*, vol. 55, pp. 284–306, 1974.

[29] D. Marcuse, "RMS width of pulses in nonlinear dispersive fibers," *Journal of Lightwave Technology*, vol. 10, no. 1, pp. 17–21, 1992.

[30] J. Santhanam and G. P. Agrawal, "Raman-induced spectral shifts in optical fibers: general theory based on the moment method," *Optics Communications*, vol. 222, no. 1-6, pp. 413–420, 2003.

[31] S. Roy and S. K. Bhadra, "Solving soliton perturbation problems by introducing Rayleigh's dissipation function," *Journal of Lightwave Technology*, vol. 26, no. 14, pp. 2301–2322, 2008.

[32] M. Scalora, M. S. Syrchin, N. Akozbek, E. Y. Poliakov, G. D'Aguanno, N. Mattiucci, M. J. Bloemer, and A. M. Zheltikov, "Generalized nonlinear Schrödinger equation for dispersive susceptibility and permeability: application to negative index materials," *Physical Review Letters*, vol. 95, no. 1, p. 013902, 2005.

[33] J. B. Pendry and D. R. Smith, "Reversing light with negative refraction," *Physics Today*, vol. 57, pp. 37–43, 2004.

[34] R. Boyd, *Nonlinear Optics*. Academic Press, 2008.

[35] H. Ticha and L. Tichy, "Semiempirical relation between non-linear susceptibility (refractive index), linear refractive index and optical gap and its application to amorphous chalcogenides," *Journal of Optoelectronics and Advanced Materials*, vol. 4, no. 2, pp. 381–386, 2002.

[36] J. Hult, "A fourth-order Runge–Kutta in the interaction picture method for simulating supercontinuum generation in optical fibers," *Journal of Lightwave Technology*, vol. 25, no. 12, pp. 3770–3775, 2007.

[37] N. Linale, J. Bonetti, A. D. Sánchez, S. Hernandez, P. I. Fierens, and D. F. Grosz, "Modulation instability in waveguides with an arbitrary frequency-dependent nonlinear coefficient," *Optics Letters*, vol. 45, no. 9, pp. 2498–2501, 2020.

[38] N. Linale, J. Bonetti, A. Sparapani, A. D. Sánchez, and D. F. Grosz, "Equation for modeling two-photon absorption in nonlinear waveguides," *Journal of the Optical Society of America B*, vol. 37, no. 6, pp. 1906–1910, 2020.

[39] A. D. Sánchez, N. Linale, J. Bonetti, and D. F. Grosz, "Modulation instability in waveguides doped with anisotropic nanoparticles," *Optics Letters*, vol. 45, no. 11, pp. 3119–3122, 2020.

[40] N. Linale, P. I. Fierens, J. Bonetti, A. D. Sánchez, S. M. Hernandez, and D. F. Grosz, "Measuring self-steepening with the photon-conserving nonlinear Schrödinger equation," *Optics Letters*, vol. 45, no. 16, pp. 4535–4538, 2020.

[41] A. K. Atieh, P. Myslinski, J. Chrostowski, and P. Galko, "Measuring the Raman time constant (T_R) for soliton pulses in standard single-mode fiber," *Journal of Lightwave Technology*, vol. 17, no. 2, pp. 216–221, 1999.

Nicolás Linale. Electronics Engineer (2017), Universidad Tecnológica Nacional (UTN), Argentina. PhD. student, Comisión Nacional de Energía Atómica (CNEA) and Consejo Nacional de Investigaciones Científicas y Técnicas (CONICET).

Pablo I. Fierens. Electronics Engineer (1997), Instituto Tecnológico de Buenos Aires (ITBA), Argentina. MSc (2000) and PhD (2003), Cornell University, USA. Fierens is Professor and director of the Optoelectronics Center at ITBA. Independent Researcher at CONICET. IEEE Senior Member. Fierens is interested in communications, nonlinear optics, and noise in nonlinear systems.

Diego F. Grosz. Licenciado degree in Physics (1993), Universidad de Buenos Aires (UBA), Argentina. PhD (1998), Universidade Estadual de Campinas, Brazil. He is currently director of the Optical Communications Group at Departamento de Ingeniería en Telecomunicaciones, CNEA, Argentina. Grosz is Independent Researcher at CONICET. His research interests include nonlinear optics and communications.